

# Artificial Neural Network based automatic classification of target shapes from GPR data

Nairit Barkataki

*Dept. of Instrumentation & USIC*  
Gauhati University  
Guwahati, India

Anirban Bhattacharjee

*Dept. of Instrumentation & USIC*  
Gauhati University  
Guwahati, India

Sharmistha Mazumdar

*Dept. of Instrumentation & USIC*  
Gauhati University  
Guwahati, India

Banty Tiru

*Dept. of Physics*  
Gauhati University  
Guwahati, India

Utpal Sarma

*Dept. of Instrumentation & USIC*  
Gauhati University  
Guwahati, India

**Abstract**—Identifying and classifying buried artefacts remains a major scientific and technological problem. Shape recognition will aid investigators in classifying buried items and narrowing down areas of interest. An artificial neural network (ANN) model for automated object shape classification using GPR data is developed in this paper. A synthetic dataset is developed using finite difference time domain (FDTD) simulation and utilised to train and evaluate the proposed ANN model. The model performs well in identifying three shapes of cylindrical, rectangular, and triangular objects.

**Index Terms**—deep learning, artificial neural network, classification, object shape, ground penetrating radar

## I. INTRODUCTION

The study and interpretation of subsurface objects is critical in archaeology, the military, civil engineering, geology, and other areas. Ground penetrating radar (GPR) is a popular choice for subsurface investigation and the detection of buried objects such as utility lines, land mines etc [1]. GPR has been widely utilised to identify subterranean structures in a non-destructive manner.

GPR has been used to uncover many ancient monuments and sculptures in different parts of the world including those of the roman, greek, indian, egyptian and chinese civilisations [2], [3], [3], [4].

The identification and classification of landmines, improvised explosive devices, tunnels, and similar objects continues to be a significant scientific and technical challenge. GPR, in conjunction with other current technologies, complements the identification of such objects since it can detect any dielectric anomalies in the soil [5].

The identification of shapes will help investigators to classify buried objects as well as narrow down regions of interests in case of archaeological excavations. It will also reduce cases of false positives when looking for landmines and other explosive devices.

Due to the difficulty in analysing GPR signals, there are two primary obstacles in revealing subterranean objects using GPR. The first is that, interpretation of GPR B-scan data still depends significantly on human efforts and trained specialists. Second, traditional GPR data processing approaches aimed at

GPR data interpretation are either conceptually complex or computationally expensive. It is imperative to develop ways for interpreting raw GPR data that are straightforward and easy to use.

Gader et al. employed a hidden markov model (HMM) to analyse hyperbolas in GPR B scans to locate landmines. [6]. Pasolli et al. presented an object detection approach in GPR data that used a novel unsupervised technique based on genetic algorithms (GA). It enabled the localisation of linear and hyperbolic patterns [7].

Of late, machine learning algorithms have proven to be a reliable option for GPR data interpretation. A machine learning based automated detection of subsurface explosives artefacts was proposed by Núñez et al. [8]. Others have demonstrated the application of machine learning algorithms for estimating the size of buried objects [9], [10].

Recently, the use of ANN has gained momentum due to greater availability of high performance computing platforms. Several studies have demonstrated that classification problems of GPR data show significant improvement in performance after using deep learning algorithms. Zhu et al. explored the difficulties of utilising deep learning techniques for remote sensing data analysis and concluded that deep learning models tend to have superior performance over classical approaches in classification and detection related problems [11]. On analysed GPR data, Kim et al. found that the proportion of misclassification dropped when deep learning techniques were used [12].

Lei et al. used Faster Region-based CNN (Faster RCNN) for GPR B-scan hyperbola detection. Compared to traditional methods, their scheme demonstrated improved accuracy and robustness in terms of real-time detection and localisation of targets. Nuaimy et al. used ANN and pattern recognition techniques to generate high resolution images of the subsurface with improved computation times which proved to be useful for on-site GPR mapping [13]. A neural network model was proposed by Senanayake et al. to estimate soil moisture in catchment areas based on remote sensing and GPR data. [14] while others have proposed models for classifying soil types [15] and estimating soil moisture [16]. SVM models were also

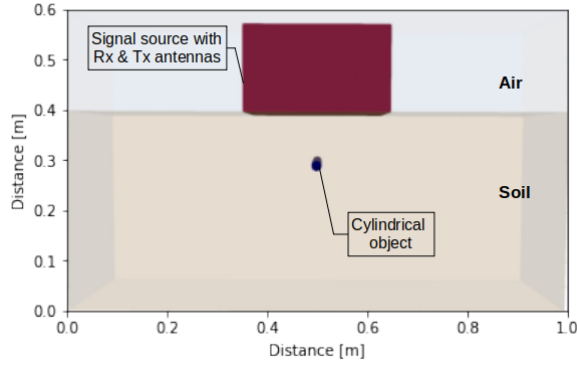


Fig. 1. Simulated model

proposed by other researchers to classify soil types [16], [17].

Although various algorithms have been developed for detecting and classification of subsurface objects, further research is needed to explore the feasibility of detecting and classifying shapes of buried objects using GPR. This paper mainly focuses on

- 1) The creation of a synthetic GPR database for target shape classification.
- 2) The development of an ANN model capable of accurately classifying target shapes using GPR data.

## II. GPR DATA

The dataset for this study is generated using gprMax, a FDTD based simulator. The dimensions of the simulated model is  $1000 \text{ mm} \times 400 \text{ mm} \times 600 \text{ mm}$  ( $X \times Y \times Z$ ). As shown in Figure 1, the top 200 mm of the model is a layer of the soil. For the soil used in this study, the suitable value for time window is found to be 14 ns.

Objects of cylindrical, triangular and rectangular shapes are assumed to be buried in the soil at depths ranging from 41 mm to 265 mm from the surface. All the objects are made up of aluminium, having relative permittivity  $\epsilon_r=10.8$  and conductivity  $\sigma = 3.5 \times 10^7 \text{ S/m}$ . The simulation parameters are given in Table I.

TABLE I  
PARAMETERS USED FOR FDTD SIMULATION

Sl. No.	Simulation Parameters	Values
1	Excitation waveform type	Gaussian
2	Antenna frequency	400 MHz
3	Time window	14 ns
4	Spatial resolution	2 mm
5	Maximum radius of cylindrical object	58 mm
6	Minimum radius of cylindrical object	7 mm
7	Maximum width of rectangular object	29 mm
8	Minimum width of rectangular object	6 mm
9	Maximum length of each side of triangular object	58 mm
10	Minimum length of each side of triangular object	7 mm

NVIDIA GPUs Tesla T4, K80 and RTX3090 are used to accelerate the simulations. Time taken for each simulation usually ranges from few seconds (RTX3090) to few minutes (K80).

Figure 2 shows the geometry and corresponding A-Scans of the models of similar object sizes at a depth of 200 mm underneath the soil surface having soil relative permittivity ( $\epsilon_r$ ) of 10 and conductivity ( $\sigma$ ) of 0.002 S/m. The value of time window is dependent on the relative permittivity of the soil. For the soil used in this study, the suitable value for time window is found to be 14 ns.

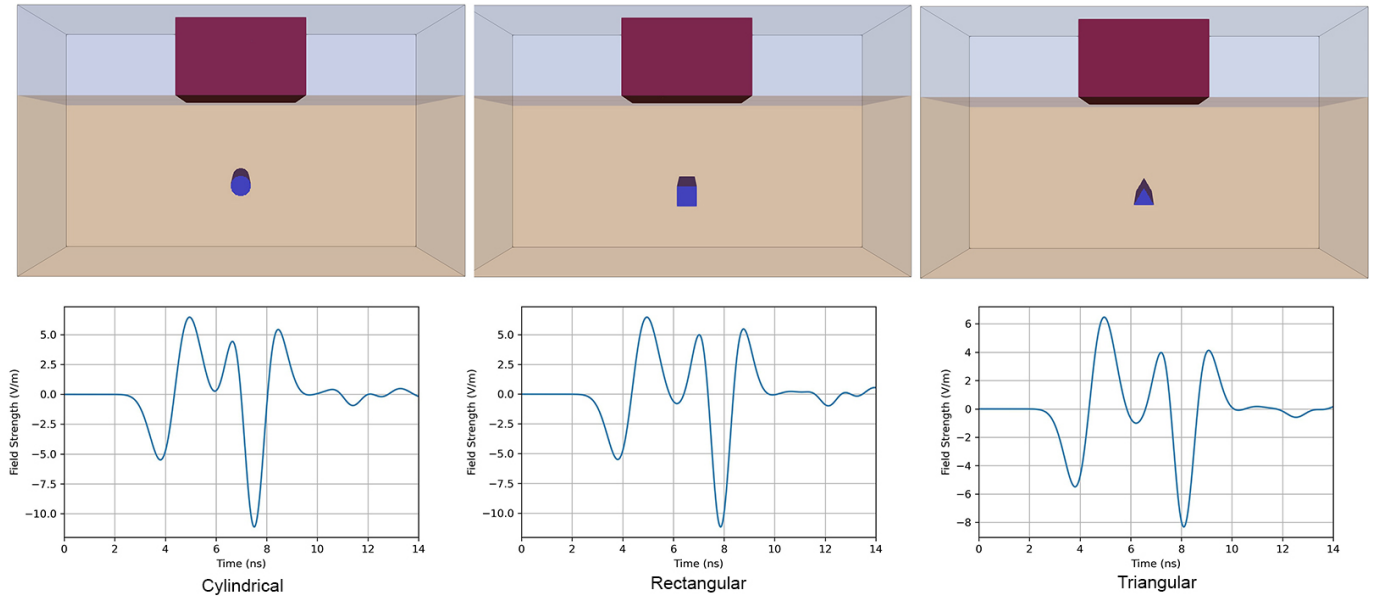


Fig. 2. Three different shapes buried inside the soil and their corresponding A-Scans

### A. Data Preprocessing

A total of 11500 A-Scans are generated for this study, each having 3631 values of amplitude across the depth of the model. For preparing the dataset for training, all the A-Scans are concatenated to form an array of dimensions  $11500 \times 3631$ , along with their respective labels (shape of the object).

## III. METHODOLOGY

In this work, ANN is used for classification of object shapes. 9200 samples (80%) are used for training and 2300 (20%) samples are used for validation and testing of the model. During the training phase, a neural network learns to classify accurately by minimising the errors. An activation function is used to define the output of each neuron and a loss function is used to monitor the error. The goal is to get the loss as near to zero as possible.

### A. The Proposed Model

Multiple training runs show that the ANN model with 5 hidden layers has the best accuracy, and the architecture is

shown in Figure 3.

The proposed model consists of 6 layers including the input layer. ReLU (Rectified Linear Unit) activation function in all the layers. The function gives 0 as output, when the input to the neuron is negative and equal to the input otherwise, as shown in 1.

$$f(n) = \max(0, n) \quad (1)$$

,where  $n$  is neuron input.

The initial number of units in the input layer is taken to be 3631, and made half for each subsequent hidden layers i.e. 3631, 1815, 907, 453, 226 and 113. The output layer containing 3 units uses softmax as the activation function to classify the three object shapes.

For optimising the model, adaptive gradient (AdaGrad) algorithm is implemented to minimise the loss function by changing the learning rate in each layer. The loss function used in the model is categorical cross-entropy.

While training the model, the validation accuracy of the model is monitored at the end of each epoch and the training

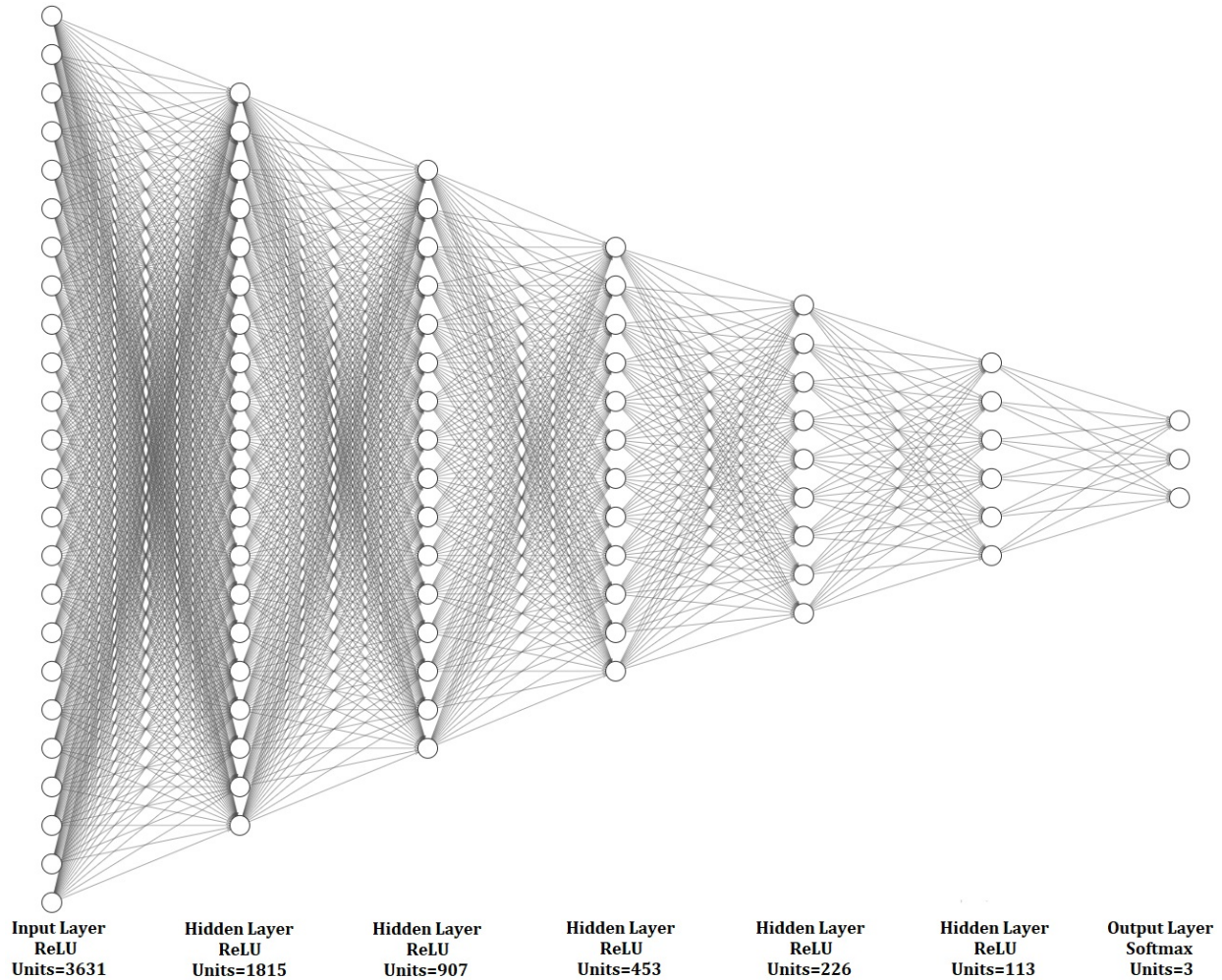


Fig. 3. Proposed ANN architecture

is terminated when no improvement is observed over a specific number epochs (patience). Figure 4 shows the training and validation accuracy of the model. The accuracy increases over 830 epochs, after which the training stops due to no further improvement in 100 successive epochs.

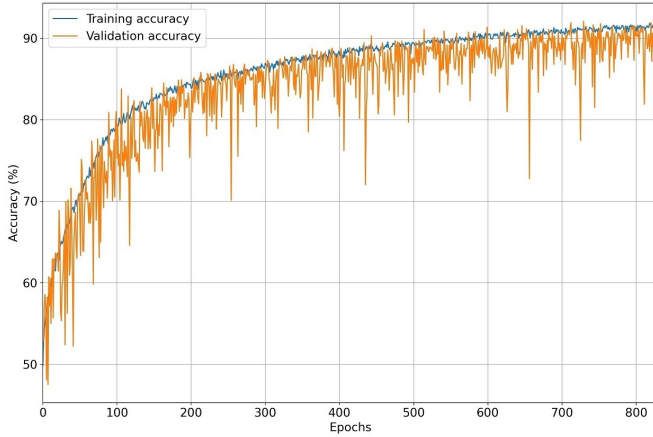


Fig. 4. Accuracy curve during training and validation of the model

To prevent overfitting of the model, dropout layers are used in neural networks. This layer randomly sets a fraction of the input neurons to zero at each step during training. In the proposed model, dropout of 20% is used in the first 3 layers. This helps in increasing the validation accuracy of the model to 92%. Without dropout, the accuracy does not increase beyond 89% during validation. The entire GPR program is written using Python and its deep learning frameworks Keras and TensorFlow.

#### IV. RESULTS

After multiple training and validation of the ANN model, it is seen that overall accuracy is 92%. To evaluate the model, different metrics such as precision, F1-score and recall are calculated corresponding to the 3 different shapes as shown in Table II. The confusion matrix of the model is shown in Figure 5 in which y-axis represents true class labels and x-axis represents the predicted class labels.

TABLE II  
CLASSIFICATION REPORT OF THE CLASSIFIER

Object Shape	Precision	F1-score	Recall	Accuracy
Cylindrical	0.87	0.89	0.88	92%
Rectangular	0.98	0.93	0.95	
Triangular	0.91	0.92	0.92	

Precision (P) is the ability of a classifier to avoid labelling a negative occurrence as positive. In Figure 5, the precision in classifying a triangular object can be calculated as shown in eq 2. Out of 823 triangular shapes, 750 are correctly classified as triangular shape.

$$Precision = \frac{750}{823} = 0.91 \quad (2)$$

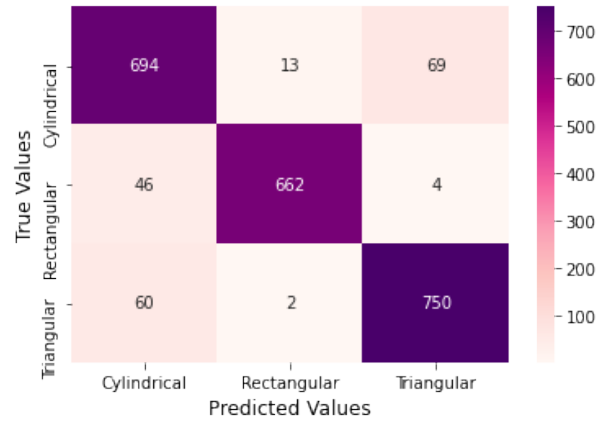


Fig. 5. Confusion matrix of the classifier

Recall (R) indicates the ability of the classifier to find all the positive instances [18]. It is calculated as the ratio of true positives to the sum of true positives and false negatives for each class as shown in eq 3.

$$Recall = \frac{750}{812} = 0.92 \quad (3)$$

F1-score is used to compare classifier models. It gives the weighted harmonic mean of precision and recall, with 1 being the best and 0 being the worst score. Considering the precision and recall for triangular shape, the F1-score can be calculated as shown in eq 4.

$$F1 = 2 \times \frac{P \times R}{P + R} = 0.92 \quad (4)$$

#### V. CONCLUSION

A novel approach for classifying object shapes based on the A-Scan data was presented in this paper. An ANN model is proposed which is used to classify object shapes from GPR A-Scan data. The overall performance of the model can be examined by analysing the classification report in Table II and confusion matrix in Figure 5.

The proposed model shows good performance in classifying three different object shapes from GPR A-Scans. In archaeological excavations, the identification of shapes will aid investigators in classifying buried artefacts and narrowing down areas of interest. When checking for landmines and other explosive devices, it will also minimise misclassifications. Moreover, application of GPR provides a non destructive approach in carrying out such surveys.

However, the dataset used to train and evaluate the proposed model has limited variation in object shapes. The authors plan to add more shapes and validate the model with experimental data.

#### VI. ACKNOWLEDGEMENT

The authors would like to acknowledge the fact that training and validating of the model would be a tremendous task without Google Colaboratory.

## REFERENCES

- [1] F. Quivira, K. Fassbender, J. A. Martinez-Lorenzo, and C. M. Rappaport, "Feasibility of tunnel detection under rough ground surfaces using underground focusing spotlight synthetic aperture radar," in *2010 IEEE International Conference on Technologies for Homeland Security (HST)*. IEEE, 2010, pp. 357–362.
- [2] S. Agrawal, M. Majumder, R. S. Bisht, and A. Prashant, "Archaeological studies at dholavira using gpr," *Curr. Sci. India*, vol. 114, p. 879, 2018.
- [3] A.-M. S. Mohamed, M. Atya, N. AbouAly, K. E. Farragawy, E. E. Hegazy, M. Saleh, K. Kabeel, and A. A. El-Mahdi, "Mapping the archaeological relics of catacombs at northeast saqqara using gpr data, egypt," *NRIAG Journal of Astronomy and Geophysics*, vol. 9, no. 1, pp. 362–374, 2020.
- [4] N. Masini, L. Capozzoli, P. Chen, F. Chen, G. Romano, P. Lu, P. Tang, M. Sileo, Q. Ge, and R. Lasaponara, "Towards an operational use of geophysics for archaeology in henan (china): Methodological approach and results in kaifeng," *Remote Sensing*, vol. 9, no. 8, p. 809, 2017.
- [5] D. J. Daniels, *Ground penetrating radar*. The Institution of Electrical Engineers, 2004.
- [6] P. D. Gader, M. Mystkowski, and Y. Zhao, "Landmine detection with ground penetrating radar using hidden markov models," *IEEE Transactions on Geoscience and Remote Sensing*, vol. 39, no. 6, pp. 1231–1244, 2001.
- [7] E. Pasolli, F. Melgani, M. Donelli, R. Attoui, and M. De Vos, "Automatic detection and classification of buried objects in gpr images using genetic algorithms and support vector machines," in *IGARSS 2008-2008 IEEE International Geoscience and Remote Sensing Symposium*, vol. 2. IEEE, 2008, pp. II–525.
- [8] X. Núñez-Nieto, M. Solla, P. Gómez-Pérez, and H. Lorenzo, "Gpr signal characterization for automated landmine and uxo detection based on machine learning techniques," *Remote sensing*, vol. 6, no. 10, pp. 9729–9748, 2014.
- [9] N. Barkataki, S. Mazumdar, R. Talukdar, P. Chakraborty, B. Tiru, and U. Sarma, "Prediction of size of buried objects using ground penetrating radar and machine learning techniques," in *2020 International Conference on Computational Performance Evaluation (ComPE)*. IEEE, 2020, pp. 781–785.
- [10] I. Giannakis, A. Giannopoulos, and C. Warren, "A machine learning scheme for estimating the diameter of reinforcing bars using ground penetrating radar," *IEEE Geoscience and Remote Sensing Letters*, 2020.
- [11] X. X. Zhu, D. Tuia, L. Mou, G.-S. Xia, L. Zhang, F. Xu, and F. Fraundorfer, "Deep learning in remote sensing: A comprehensive review and list of resources," *IEEE Geoscience and Remote Sensing Magazine*, vol. 5, no. 4, pp. 8–36, 2017.
- [12] N. Kim, S. Kim, Y.-K. An, and J.-J. Lee, "Triplanar imaging of 3-d gpr data for deep-learning-based underground object detection," *IEEE Journal of Selected Topics in Applied Earth Observations and Remote Sensing*, vol. 12, no. 11, pp. 4446–4456, 2019.
- [13] W. Al-Nuaimy, Y. Huang, M. Nakhkash, M. Fang, V. Nguyen, and A. Eriksen, "Automatic detection of buried utilities and solid objects with gpr using neural networks and pattern recognition," *Journal of applied Geophysics*, vol. 43, no. 2-4, pp. 157–165, 2000.
- [14] I. Senanayake, I.-Y. Yeo, J. Walker, and G. Willgoose, "Estimating catchment scale soil moisture at a high spatial resolution: Integrating remote sensing and machine learning," *Science of The Total Environment*, vol. 776, p. 145924, 2021.
- [15] N. Barkataki, S. Mazumdar, P. B. D. Singha, J. Kumari, B. Tiru, and U. Sarma, "Classification of soil types from GPR B scans using deep learning techniques," in *2021 6th IEEE International Conference on Recent Trends in Electronics, Information & Communication Technology (RTEICT 2021)*, August 2021, pp. 840–844.
- [16] M. Malajner, D. Gleich, and P. Planinsic, "Soil type characterization for moisture estimation using machine learning and uwb-time of flight measurements," *Measurement*, vol. 146, pp. 537–543, 2019.
- [17] P. Taneja, H. K. Vasava, P. Daggupati, and A. Biswas, "Multi-algorithm comparison to predict soil organic matter and soil moisture content from cell phone images," *Geoderma*, vol. 385, p. 114863, 2021.
- [18] J. Davis and M. Goadrich, "The relationship between precision-recall and roc curves," in *Proceedings of the 23rd international conference on Machine learning*, 2006, pp. 233–240.